Crystalline vanadium (II) fluoride, VF2. Preparation, structure, heat capacity from 5 to 300 °K and magnetic ordering

J. W. Stout and W. O. J. Boo

Citation: The Journal of Chemical Physics **71**, 1 (1979); doi: 10.1063/1.438115
View online: http://dx.doi.org/10.1063/1.438115
View Table of Contents: http://scitation.aip.org/content/aip/journal/jcp/71/1?ver=pdfcov
Published by the AIP Publishing

Crystalline vanadium (II) fluoride, VF_2. Preparation, structure, heat capacity from 5 to 300 °K and magnetic ordering

J. W. Stout and W. O. J. Boo[a)]

Department of Chemistry and James Franck Institute, University of Chicago, Chicago, Illinois 60637
(Received 2 March 1979; accepted 27 March 1979)

Crystalline VF_2 was prepared by the reduction of VF_3 in an atmosphere of 3 H_2:1 HF at 1100 °C. The VF_2 formed deep blue crystalline needles. The crystal structure is of the rutile type, space group $P4_2/mnm$. Parameters determined by x-ray diffraction are $a = 4.804 \pm 0.005$ Å, $c = 3.237 \pm 0.005$ Å, $u = 0.306 \pm 0.005$. The low temperature heat capacity of VF_2 is reported from 5 to 300 °K. A sharp peak in heat capacity associated with the development of long-range magnetic order is observed at 7 °K. Smoothed values of the total heat capacity, entropy, enthalpy, and Gibbs energy are tabulated between 5 and 300 °K. Values at 298.15 °K are: $C°_P = 15.10$ cal °K^{-1} $mole^{-1}$, $S° = 18.217$ cal °K^{-1} $mole^{-1}$, $H° - H°_0 = 2661.0$ cal $mole^{-1}$. By a corresponding states approximation the magnetic contributions to the heat capacity and entropy are calculated. The magnetic heat capacity has a gradual maximum at 26.8 ±1 °K. The heat capacity curve agrees with that calculated for a one-dimensional chain with antiferromagnetic Heisenberg interactions. A value of the exchange constant, $J/k = -9.4 \pm 0.4$ °K is obtained.

In earlier papers from this laboratory low temperature heat capacity measurements of the divalent transition-metal fluorides of the rutile structure, MnF_2,[1] FeF_2,[2] CoF_2,[2] NiF_2,[3] and ZnF_2[4] have been reported. The following paper[5] presents heat capacity data of CrF_2 and CuF_2. With the exception of diamagnetic ZnF_2 each of these compounds exhibits heat capacity anomalies associated with the antiferromagnetic ordering of the magnetic moments of the transition metal ions. At the time this research was initiated the crystalline compound VF_2 was unknown and there was considerable doubt that it would be stable with respect to disproportionation into the metal and VF_3. Hydrates of VF_2 had been reported.[6]

This paper reports the preparation of crystalline VF_2, the determination of its crystal structure, and the measurement of its low-temperature heat capacity from 5 to 300 °K. A preliminary report of this work has been published.[7] VF_2 has since been prepared and characterized by Shafer,[8] by Cros, Feurer, and Pouchard,[9] and by Wanklyn, Gerrard, Wondre, and Davidson.[10]

EXPERIMENTAL

Preparation of VF_2

When HF gas was passed over metallic vanadium at a temperature of about 1250 °C a few needlelike crystals, deep blue in color, were found in that part of the graphite-lined nickel furnance tube that was about 1150 °C. Light green VF_3 was present in large amounts next to the VF_2 in a slightly cooler part of the furnace. The deep blue crystals were identified by x rays as VF_2 and a procedure was developed to reduce VF_3 to VF_2 but not metallic vanadium in a H_2–HF atmosphere.

Vancoram vanadium metal, stated by the manufacturer to be 99.79% V by weight, and to contain, in weight percent, C 0.04, Fe 0.025, N 0.039, O 0.080, H 0.054, and trace amounts of Ca, S, Si, Cr, and Mo was the starting material. One-hundred g of V in a graphite boat was heated in the furnace tube to 1250 °C in a stream of N_2 gas. The N_2 gas flow was then replaced by anhydrous HF gas and the temperature maintained at 1250 °C for 12 h. The V metal was converted to green VF_3 which had volatilized and collected in the furnace tube where the temperature was approximately 1100 °C.

The VF_3 was pulverized and passed through an 80 mesh screen. About 50 g was added to a clean graphite boat placed in the furnace tube. By trial we found that a mixture of $3H_2$ to 1HF, passed over the VF_3 sample for 8 h at 1100 °C, reduced the VF_3 to VF_2. The VF_2 consisted of interlocked needlelike crystals 0.1–0.3 mm in diameter and 1–5 mm long.

The sample of VF_2 used for the heat capacity measurements weighed 224.96 g *in vacuo*. It was a composite of seven batches prepared as described above, which were analyzed spectrochemically for trace impurities and chemically for vanadium by titration of V^{4+} with standardized $KMnO_4$ solution. The spectrochemical analysis showed 0.005 wt. % Mg, Cu, and Mn. Fe, Ni, Co, Al, Si, Na, and K were not detected. The chemical analysis of the seven batches, in weight percent V, was 57.25, 57.24, 57.24, 57.19, 57.26, 57.27, and 57.26 with a weighted mean of 57.24. The calculated weight percent of V in VF_2 is 57.28.

X-ray determination of crystal structure of VF_2

Debye–Scherrer powder photographs of VF_2 were similar in pattern and intensity to those of other fluorides[11] of the rutile structure and led to the identification of the structure of VF_2 as space group $P4_2/mnm$ with two VF_2 in a tetragonal unit cell. Table I lists the observed values of $(\sin^2\theta)/\lambda^2$ of powdered VF_2 for two films exposed in a 9 cm diameter Debye–Scherrer camera. A rotating crystal film was obtained by mounting

[a)]Present address: Department of Chemistry, University of Mississippi, University, Miss. 38677.

 0021-9606/79/010001-08$01.00

TABLE I. Debye–Scherrer x-ray data for powdered VF_2. Cu$K\alpha$ radiation. 294±3°K. Calculated line positions and intensities with $a = 4.804$ Å, $c = 3.237$ Å, $u = 0.306$. Observed intensities are visual estimates, S^+ (very strong) to W^{--} (very very weak).

Miller indices *hkl*	Film No. 5 $(\sin^2\theta)/\lambda^2$ (Å^{-2})	Film No. 5 Intensity	Film No. 6 $(\sin^2\theta)/\lambda^2$ (Å^{-2})	Film No. 6 Intensity	Calculated $(\sin^2\theta)/\lambda^2$ (Å^{-2})	Calculated Relative intensity
110	0.0221	S^+	0.0217	S^+	0.02167	1205
101	0.0351	M^+	0.0336	M	0.03469	524
200					0.04333	54
111	0.0461	M^-	0.0455	W	0.04552	345
210	0.0549	W^-	0.0546	W^-	0.05416	117
211	0.0791	S	0.0797	S	0.07802	775
220	0.0872	M	0.0877	W	0.08666	225
002	0.0961	W^-	0.0962	W^-	0.09544	135
310	0.1094	W^-	0.1086	W^-	0.10833	91
221					0.11052	11
112	0.1179	W	0.1177	W	0.11710	145
301	0.1226	M	0.1215	M	0.12135	288
311					0.13219	18
202					0.13877	23
320					0.14082	4
212					0.14960	23
321	0.1650	W^-	0.1656	W^-	0.16468	44
400	0.1746	W^-	0.1739	W^{--}	0.17332	34
222	0.1833	W	0.1826	W^-	0.18210	95
410					0.18415	16
330	0.1964	W^-	0.1950	W^{--}	0.19499	49
312	0.2043	W^-	0.2043	W^{--}	0.20376	59
411	0.2090	W	0.2081	W^{--}	0.20801	78
420	0.2179	W^-	0.2169	W^{--}	0.21665	34
331					0.21885	<1
103					0.22556	24
322					0.23626	2
113					0.23640	9
421					0.24051	9
430					0.27082	2
402 213	0.2693	M	0.2693	M	0.26876 0.26890	38 84
412					0.27959	16
510	0.2822	W	0.2814	W^{--}	0.28165	44
332	0.2905	W	0.2905	W^{--}	0.29042	62
431 501	0.2948	W	0.2948	W^{--}	0.29467 0.29467	73 7
511					0.30551	<1
223					0.30139	2
520					0.31415	<1
422 303	0.3123	M	0.3123	W^-	0.31209 0.31223	56 68
313					0.32306	4
521	0.3380	M	0.3385	W	0.33801	132
440	0.3457	W^{--}			0.34664	19
323	0.3554	W^-	0.3548	W^{--}	0.35556	34
530					0.36831	14
432					0.36625	5
441					0.37050	10
512	0.3773	M	0.3773	W	0.37708	125
004					0.38175	27
600					0.38997	42
531					0.39217	<1
413	0.3989	M^-	0.3992	W^-	0.39889	122
610					0.40081	10
114	0.4035	W	0.4036	W^{--}	0.40341	81
522					0.40958	<1

a single crystal needle of VF_2, about 0.2 mm in diameter, in the Debye–Scherrer camera. The needle was rotated about its long axis and the observed positions of the spots (Table II) show that this axis is the c axis of the crystal. The film was wrapped in 0.01 mm thick aluminum foil to minimize blackening by fluorescent

TABLE II. X-ray data for single crystal needle of VF_2 rotated about the c axis in a Debye–Scherrer camera. Cu$K\alpha$ radiation. 294 ± 3 °K. Observed intensities are visual estimates, S^+ (very strong) to W^- (very weak). Calculated intensities with $u = 0.306$. See Table I for calculated values of $(\sin^2\theta)/\lambda^2$.

Miller indices hkl	Observed $(\sin^2\theta)/\lambda^2$ (Å^{-2})	Observed intensity	Calculated relative intensity
110	0.0217	S^+	274
200	0.0431	M^-	17
210	0.0542	S	42
220	0.0867	S	106
310	0.1083	S	46
320	0.1409	W^-	2
400	0.1733	M	22
410	0.1840	M^-	11
330	0.1945	M	33
420	0.2169 α_1 0.2168 α_2	M	24
430	0.2712 α_1 0.2707 α_2	W^-	2
510	0.2818 α_1 0.2818 α_2	M^+	36
520	...	...	0.1
440	0.3470 α_1 0.3470 α_2	M	17
530	0.3683 α_1 0.3683 α_2	M	13
600	0.3900 α_1 0.3900 α_2		41
610	0.4008 α_1 0.4007 α_2	M^-	10

radiation. Cu radiation with Ni filter was used for all films.

The lattice parameter a was determined by extrapolating to $\theta = 90°$ a linear plot of $1/(4a^2)$ determined from the data of Table II versus $\cos^2\theta$. Using this value of a, the parameter c was determined from a similar extrapolation of the data from powder films 5 and 6. The values of the parameters obtained and their estimated errors are $a = 4.804 \pm 0.005$ Å, $c = 3.237 \pm 0.005$ Å. The density calculated from the parameters, 3.954 ± 0.007 g cm^{-3}, agrees with the reported[9] measured value of 3.92 ± 0.05. The most accurate determination[12] of the lattice parameters of VF_2, $a = 4.8023$ Å and $c = 3.2359$ Å at 298 °K, was made on one of our needle crystals after the completion of this work.

In the rutile structure the fluorine positions are determined by a parameter u which falls between 0.30 and 0.32 in the the other rutile fluorides.[11] The qualitative intensity data in Tables I and II shows that u of VF_2 is in this range. For the relative calculated intensities listed in Tables I and II the atomic scattering factors were corrected for temperature by factors $\exp(-B\sin^2\theta/\lambda^2)$. The values used, $B_V = 0.37$ and $B_F = 0.70$, are those found by Haefner[13] for NiF_2 at room temperature. The calculated intensities are corrected for Lorentz polarization factors appropriate for powder or rotating crystal films but not for absorption. The ratio of two weak lines, 202 and 311, is particularly sensitive to the value of u and has been used[11] to determine it. Since neither of these lines was observed in the films of Table I, two additional overexposed films were taken of a powdered sample of VF_2 cemented on the outside of a thin glass rod. The relative intensities of four lines, 311, 202, 400, and 420, were measured on these films by comparison with a calibration film with various timed exposures. For a range of u values, intensities calculated as in Table I with an additional factor to correct for absorption[14] were computed and compared with the observed values. A value $u = 0.306 \pm 0.005$ was obtained.

Calorimetric apparatus

The calorimeter, laboratory designation A, and platinum thermometer-heater, laboratory designation T6 have been described previously.[3,15] The recalibration of the thermometer from 10 to 300 °K was recently described.[1] In order to extend the calibration of the thermometer down to 5 °K its resistance was measured at the boiling point of helium. From this and the data of de Haas and de Boer[16] on the separation of the resistance of Pt into the sum of residual and "ideal" parts we constructed a temperature scale between 5 to 10 °K which blended smoothly into the scale above 10 °K. We estimate the possible error in temperature below 10 °K as 0.1 °K. Details are given in the thesis[17] of one of us. The calibration of the thermometer was checked at the boiling point of H_2 before and after the measurements on VF_2. For heat capacity measurements below 10 °K the cryostat Dewar was filled with liquid helium and the cryostat was immersed in a case containing liquid nitrogen.

Experimental results

Table III lists the experimental measurements of the heat capacity of VF_2. The accuracy of the heat capacity data is estimated as 5% at 6 °K, 2% at 10 °K, 1% at 20 °K, increasing to 0.2% between 40 and 200 °K and decreasing to 0.5% at 300 °K. The temperature T_{av} is the arithmetic mean of the initial and final temperatures. The approximate temperature rise ΔT of each measurement is also listed. The heat capacities listed are values of $\Delta H/\Delta T$ and curvature corrections have not been applied. 1 cal = 4.184 J. The measurements are listed in chronological order. No evidence of thermal hysteresis or slowness in the attainment of equilibrium was observed.

After the completion of the measurements of Series I, II, and III we realized that, although no peak in heat capacity indicating the onset of long-range magnetic order had been found above 10 °K, the unusually large heat capacity between 10 and 20 °K indicated loss of magnetic entropy and would make questionable the usual extrapolation to 0 °K. Series IV and V extend the measurements down to 5 °K. A sharp peak in heat capacity was found at 7.0 ± 0.1 °K. The data of Series IV and V were measured with a thermometer current of 3.3 mA, and those of Series VI, measurements with small temperature rise to define the shape of the peak, with a current of 15 mA. At temperatures above 10 °K the maximum current used was 2.4 mA. The heat capacity of VF_2

TABLE III. Heat capacity of VF_2.

0 °C = 273.15 °K Molecular weight = 88.939

T_{av} (°K)	Approx. ΔT, (°K)	$\Delta H/\Delta T$ (cal °K^{-1} mole^{-1})	T_{av} (°K)	Approx. ΔT, (°K)	$\Delta H/\Delta T$ (cal °K^{-1} mole^{-1})
	Series I				
52.41	5.02	3.067	21.69	1.66	1.507
56.96	4.05	3.369	23.58	2.10	1.608
60.99	3.99	3.657	25.46	2.08	1.698
64.71	3.93	3.933	27.46	1.98	1.791
68.59	3.84	4.217	29.66	2.40	1.884
72.38	3.74	4.508	31.95	2.17	1.983
76.28	4.04	4.794	34.27	2.49	2.089
80.40	4.18	5.113	36.93	2.83	2.207
84.20	4.31	5.412	39.91	3.15	2.346
88.73	4.75	5.765	43.49	4.01	2.533
93.60	4.97	6.135	47.63	4.27	2.768
98.62	5.11	6.505		Series III	
103.72	5.09	6.885	299.68	6.54	15.13
108.98	5.40	7.269		Series IV	
114.18	5.68	7.650	5.585	0.272	0.36
119.73	5.37	8.037	5.997	0.486	0.47
125.31	5.77	8.426	6.455	0.366	0.64
131.19	5.97	8.819	6.775	0.277	0.86
136.95	5.56	9.196	6.999	0.179	1.36
142.77	6.05	9.554	7.311	0.459	0.53
148.88	6.12	9.926	7.783	0.491	0.51
155.29	6.68	10.30	8.262	0.499	0.52
162.12	6.59	10.66	8.680	0.495	0.54
169.09	7.22	11.02	9.182	0.485	0.58
176.27	7.00	11.38	9.663	0.480	0.61
183.17	6.63	11.69		Series V	
190.14	6.79	12.01	5.297	0.315	0.31
198.28	7.34	12.33	5.604	0.268	0.37
205.17	7.01	12.59	6.388	0.763	0.614
212.73	7.52	12.86	6.828	0.117	0.90
220.24	7.19	13.12	6.932	0.099	1.07
230.34	7.54	13.45	7.003	0.051	2.10
238.01	7.22	13.69	7.098	0.140	0.77
245.63	7.63	13.90	7.272	0.214	0.50
253.50	7.33	14.10	7.633	0.511	0.49
260.88	7.73	14.29	8.36	0.992	0.525
269.04	7.43	14.48	9.49	0.960	0.598
276.94	7.76	14.68	10.49	0.949	0.672
285.31	7.49	14.85	11.45	0.958	0.750
293.34	7.81	15.00		Series VI	
	Series II		6.658	0.147	0.71
10.62	0.262	0.681	6.801	0.085	0.78
10.96	0.412	0.711	6.870	0.042	0.88
11.47	0.605	0.751	6.930	0.038	0.98
12.15	0.732	0.805	6.976	0.033	1.13
12.90	0.755	0.869	7.013	0.029	1.29
13.66	0.789	0.936	7.043	0.019	1.95
14.48	0.841	1.005	7.061	0.012	3.1
15.36	0.912	1.079	7.087	0.030	1.24
16.32	1.01	1.154	7.135	0.047	0.80
17.40	1.15	1.236	7.198	0.059	0.64
18.66	1.36	1.319	7.328	0.135	0.50
20.19	1.67	1.417	7.507	0.200	0.54

between 5 and 10 °K is shown in Fig. 1. It is apparent that long-range magnetic order begins at 7 °K and that the total entropy at this temperature is small compared to $R\ln 4$, the total magnetic entropy expected for the V^{2+} ion.

DISCUSSION

Thermodynamic properties

Table IV lists smoothed values of the heat capacity, entropy, enthalpy, and Gibbs energy of VF_2. The values

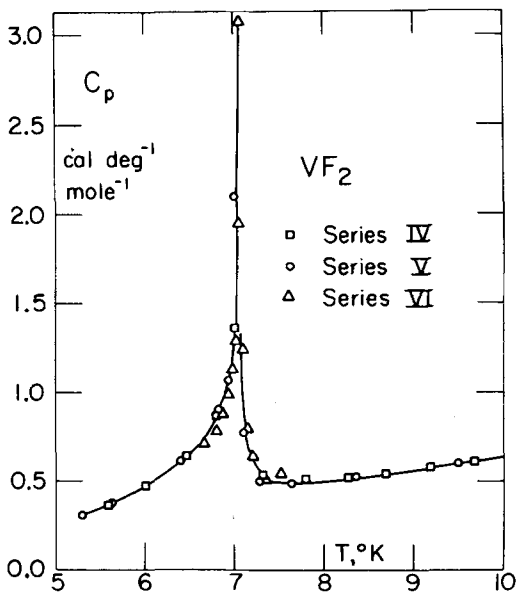

FIG. 1. Molal heat capacity of VF_2 between 5 and 10 °K.

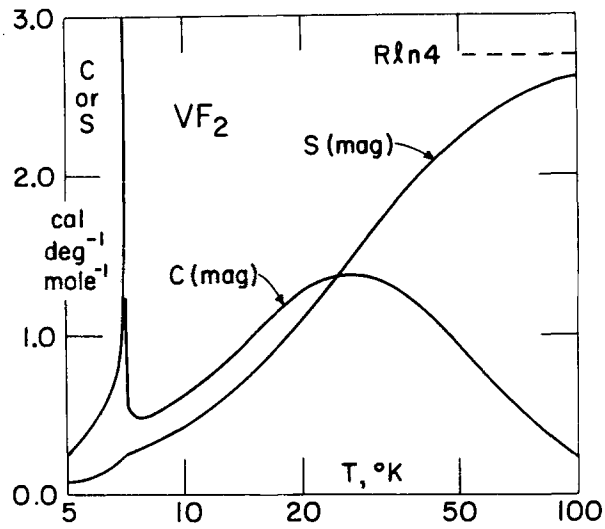

FIG. 3. Magnetic contributions to the molal heat capacity and entropy of VF_2 vs temperature (logarithmic scale).

of $\Delta H/\Delta T$ were corrected[18] for curvature before smoothing. The extrapolation to 0 °K was made on plots of $C_P T^{-2}$ and $C_P T^{-3}$ vs T. Values of thermodynamic functions from 5 to 10 °K were calculated from a graph of C_P vs T. Between 6.8 and 7.2 °K values of ΔH for each series were obtained by summing the individual values of successive measurements and values of ΔS were obtained by summing $\Delta H/T$. Values obtained from Series IV, V, and VI respectively are: ΔH, 0.406, 0.402, and 0.446 cal mole^{-1}; ΔS, 0.058, 0.058, and 0.064 cal °K^{-1} mole^{-1}. From 10 to 300 °K the thermodynamic functions were obtained from fits of the observed C_P data to polynomials in T with computer programs POLYFIT and THFNS.

Magnetic contributions to the heat capacity of VF_2

We have estimated the lattice heat capacity from the corresponding states approximation using the heat capacity of the isomorphic diamagnetic ZnF_2 as a reference.[4] In Fig. 2 values of $r(VF_2, C_P)$ and $r(VF_2, S)$ are plotted versus temperature. For V^{2+} the ground electronic state in an octahedral field is an orbital singlet with a spin of $\frac{3}{2}$. The high-temperature value of the magnetic contribution to the entropy is therefore $S_\infty = R \ln 4$. We recall that $r(VF_2, S) = T'/T$ and $r(VF_2, C_P) = T''/T$ where T' is the temperature where the entropy of ZnF_2 is equal to $S_T - S_\infty$ of VF_2 at T, and T'' is the temperature where the heat capacity of ZnF_2 equals that of VF_2 at T. As the temperature is lowered the increase in C(mag) and $(S_\infty - S_T)$(mag) causes $r(MF_2, C_P)$ to rise and $r(MF_2, S)$ to fall as is illustrated in Fig. 2. Boo and Stout[1] took advantage of the fact that at high temperatures C(mag) $= AT^{-2}$ and $(S_\infty - S_T)$(mag) $= \frac{1}{2} AT^{-2}$ where A is a constant. At high temperatures one may therefore obtain r values by subtracting AT^{-2} from C_P and adding $\frac{1}{2} AT^{-2}$ to $S_T - S_\infty$(mag). The value of A is adjusted until the corrected $r(VF_2, C_P)$ and $r(VF_2, S)$ coincide. The value at coincidence is called $r(VF_2, A)$. Values of $r(VF_2, A)$ for temperatures above 60 °K are shown as triangles in Fig. 2. Between 60 and 180 °K, $r(VF_2, A)$ is nearly constant. We have chosen the value $r(VF_2, A) = 0.869 \pm 0.005$. Over this temperature range A varies from 2.3 to 2.8×10^3 cal °K mole^{-1}. The mean value is 2.6×10^3 cal °K mole^{-1}.

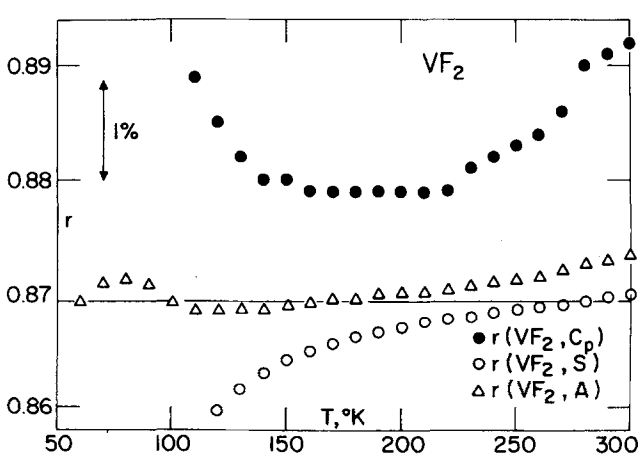

FIG. 2. Corresponding states ratios, r, for VF_2 compared to ZnF_2 vs temperature. See text for definitions.

The values of C_P(lat) and S(lat) of VF_2 at temperature T are therefore values of C_P and S of ZnF_2 at temperature $0.869T$. By subtracting C_P(lat) from C_P and S(lat) from S the values of C(mag) and S(mag) of VF_2 are obtained. In Table V values of the magnetic contributions to the heat capacity and entropy of VF_2 are calculated. C(mag) and S(mag) of VF_2 are shown graphically in Fig. 3. The energy of the magnetic interactions, E(mag), between 0 °K and infinite temperature was obtained as follows. The energy at 10 °K is the $H^\circ - H_0^\circ$ value from Table IV less a lattice contribution of 0.07 cal mole^{-1}. The contribution between 10 and 100 °K was obtained by numerical integration of the C(mag) values in Table V. The contribution above 100 °K was obtained by integration of $C(\text{mag}) = 2.6 \times 10^3\, T^{-2}$. The sum of the contributions is $E(\text{mag}) = 101 \pm 5$ cal mole^{-1}.

The peak in heat capacity at 7 °K shown in Fig. 3

TABLE IV. Thermodynamic properties of VF_2.

T (°K)	C_P° (cal °K^{-1} mole^{-1})	S° (cal °K^{-1} mole^{-1})	$H^\circ - H_0^\circ$ (cal mole^{-1})	$-\frac{(G^\circ - H_0^\circ)}{T}$ (cal °K^{-1} mole^{-1})
5	0.25	0.076	0.29	0.018
6	0.47	0.139	0.64	0.032
7	3.	0.248	1.36	0.054
8	0.51	0.329	1.96	0.084
9	0.56	0.394	2.49	0.117
10	0.632	0.455	3.09	0.146
15	1.050	0.789	7.28	0.304
20	1.406	1.142	13.46	0.469
25	1.677	1.486	21.20	0.638
30	1.899	1.812	30.15	0.807
35	2.119	2.121	40.19	0.973
40	2.352	2.419	51.36	1.135
45	2.617	2.711	63.77	1.294
50	2.913	3.002	77.59	1.450
55	3.236	3.295	92.95	1.605
60	3.585	3.591	110.0	1.758
65	3.950	3.892	128.8	1.911
70	4.325	4.199	149.5	2.063
75	4.705	4.510	172.1	2.216
80	5.088	4.826	196.6	2.369
85	5.474	5.147	223.0	2.523
90	5.858	5.470	251.3	2.678
95	6.239	5.797	281.5	2.833
100	6.614	6.127	313.7	2.990
110	7.347	6.791	383.5	3.305
120	8.058	7.461	460.6	3.624
130	8.742	8.133	544.5	3.944
140	9.389	8.805	635.3	4.267
150	9.991	9.474	732.2	4.592
160	10.55	10.136	835.0	4.918
170	11.07	10.792	943.0	5.245
180	11.55	11.438	1056.2	5.571
190	11.99	12.075	1173.9	5.896
200	12.40	12.700	1295.8	6.221
210	12.77	13.314	1421.7	6.544
220	13.12	13.916	1551.1	6.866
230	13.44	14.506	1683.9	7.185
240	13.74	15.085	1819.8	7.502
250	14.01	15.651	1958.6	7.817
260	14.27	16.206	2100.0	8.129
270	14.51	16.749	2243.9	8.438
280	14.74	17.281	2390.2	8.744
290	14.94	17.802	2538.6	9.048
300	15.13	18.311	2689.0	9.348
273.15	14.59	16.923	2289.7	8.534
298.15	15.10	18.217	2661.0	9.293

marks the beginning of long-range order and the substantial magnetic heat capacity above this temperature indicates large short-range correlation of the spins of the V^{2+} ions. At 7 °K the magnetic contribution to the entropy is only 8.9% of $R\ln 4$ and the magnetic energy of 1.34 cal mole^{-1} is only 1.3% of its high temperature limit. In the rutile structure there are two exchange couplings between near neighbors. An exchange constant J_1 couples an ion to two neighbors at [001] and $[00\bar{1}]$ which are at a distance c(3.237 Å in VF_2) from the central ion. J_2 couples the central ion to eight neighbors at $[\pm\frac{1}{2}, \pm\frac{1}{2}, \pm\frac{1}{2}]$ at a distance 3.763 Å. In MnF_2, FeF_2, CoF_2, and NiF_2 $J_2 < 0$ (antiferromagnetic) and $|J_1| < |J_2|$. The long-range ordering in these compounds is three-dimensional. If in VF_2 J_2 were zero and $J_1 < 0$ the magnetic interactions would be those of independent linear chains parallel to the c axis with antiferromagnetic coupling between neighboring V^{2+} ions. Such a one-dimensional array of ions with short-range interactions does not develop long-range order at $T > 0$ °K. Magnetic susceptibility data[19] show that in VF_2 the preponderant interactions are antiferromagnetic. These considerations led us to suggest[7] that in VF_2 J_1 is negative and is greater in magnitude than J_2. The interactions between chains (J_2) causes the onset of three-dimensional order at 7 °K, but above this temperature the magnetic and thermal properties would be almost those of an antiferromagnetically coupled one-di-

TABLE V. Magnetic contributions to the heat capacity and entropy of VF_2.

T (°K)	C_P	C_P(lat)	C(mag)	S	S(lat)	S(mag)	$\frac{S(\text{mag})}{R \ln 4}$
				(cal °K^{-1} mole^{-1})			
5	0.25	0.002	0.25	0.076	0.001	0.075	0.027
6	0.47	0.003	0.47	0.139	0.001	0.138	0.050
7	3	0.005	3	0.248	0.002	0.246	0.089
8	0.51	0.008	0.50	0.329	0.003	0.326	0.118
9	0.56	0.011	0.55	0.394	0.004	0.390	0.142
10	0.632	0.016	0.616	0.455	0.005	0.450	0.163
15	1.050	0.054	0.996	0.789	0.018	0.771	0.280
20	1.406	0.146	1.260	1.142	0.044	1.098	0.399
25	1.677	0.310	1.367	1.486	0.093	1.393	0.506
30	1.899	0.545	1.354	1.812	0.168	1.644	0.597
35	2.119	0.848	1.271	2.121	0.274	1.847	0.670
40	2.352	1.195	1.157	2.419	0.410	2.009	0.729
45	2.617	1.578	1.039	2.711	0.573	2.138	0.776
50	2.913	1.990	0.923	3.002	0.761	2.241	0.813
55	3.236	2.417	0.819	3.295	0.970	2.325	0.844
60	3.585	2.862	0.723	3.591	1.199	2.392	0.868
65	3.950	3.317	0.633	3.892	1.446	2.446	0.888
70	4.325	3.771	0.554	4.199	1.709	2.490	0.904
75	4.705	4.221	0.484	4.510	1.985	2.525	0.917
80	5.088	4.656	0.432	4.826	2.271	2.555	0.927
85	5.474	5.091	0.383	5.147	2.566	2.581	0.937
90	5.858	5.526	0.332	5.470	2.870	2.600	0.944
95	6.239	5.960	0.279	5.797	3.179	2.618	0.950
100	6.614	6.377	0.237	6.127	3.496	2.631	0.955

mensional chain.

The Hamiltonian for a one-dimensional chain of N atoms of spin quantum number S, with exchange coupling constant J between nearest neighbors, and with crystal field parameters D and E is

$$\mathcal{H} = -2J \sum_{i=1}^{N-1} S_{z,i} S_{z,i+1} + \gamma (S_{x,i} S_{x,i+1} + S_{y,i} S_{y,i+1}) + \sum_{i=1}^{N} D[S_{z,i}^2 - \tfrac{1}{3} S(S+1)] + E(S_{x,i}^2 - S_{y,i}^2) \ . \quad (1)$$

When $\gamma = 1$ and D and E are zero the isotropic Heisenberg model is obtained and when $\gamma = D = E = 0$ the Hamiltonian describes the Ising model. The measurements of Peter and Mock[20] on the paramagnetic resonance of dilute V^{2+} in ZnF_2 obtained $D = 0.425$ cm^{-1}, $|E| = 0.153$ cm^{-1}, consistent with the small anisotropy of the magnetic susceptibility[19] of VF_2. The crystal field parameters are small in magnitude compared to the exchange interactions needed to describe the observed magnetic heat capacity in VF_2 and we therefore expect the principal features of the curves shown in Fig. 3 to be describable by an isotropic one-dimensional antiferromagnetic Heisenberg chain.

In Table VI we have compared the values of (C/R)(mag) for VF_2 obtained from our corresponding states analysis with those calculated for the Ising model and the antiferromagnetic Heisenberg model. The observed gradual maximum in (C/R) is 0.689 at 26.8 °K. The entries for the Ising and Heisenberg models in Table VI were calculated with J values to make their heat capacity a maximum at 26.8 °K. The one-dimensional Ising model has long been solved[21] exactly. For $S = \frac{1}{2}$ the partition function in zero magnetic field is

$$Z = \{\cosh 9K + \cosh K + [(\cosh 9K - \cosh K)^2 + (2\cosh 3K)^2]^{1/2}\}^N \ , \quad (2)$$

where $K = |J|/(2kT)$. The heat capacity is

$$(C/R)(\text{mag}) = K^2(\partial^2 \ln Z / \partial K^2) \ . \quad (3)$$

We have calculated the values for the Ising model listed

TABLE VI. Comparison of magnetic contributions to C/R of VF_2 with those calculated for a one-dimensional antiferromagnetic linear chain with Heisenberg and Ising interactions.

T (°K)	(C/R)(mag) Observed VF_2	Ising $(J/k) = -11.55$ °K	Heisenberg[a] $(J/k) = -9.81$ °K
10	0.310	0.059	0.279
15	0.501	0.393	0.484
20	0.634	0.923	0.604
25	0.688	1.243	0.655
30	0.681	1.210	0.646
35	0.640	1.007	0.612
40	0.582	0.790	0.565
45	0.523	0.614	0.513
50	0.464	0.482	0.461
55	0.412	0.384	0.413
60	0.364	0.312	0.370
65	0.319	0.258	0.332
70	0.279	0.216	0.298
75	0.244	0.184	0.268
80	0.217	0.158	0.242
85	0.193	0.137	0.220
90	0.167	0.121	0.200
95	0.140	0.107	0.182
100	0.119	0.095	0.165

[a]Reference 23(a).

in Table VI with the above expressions and $J/k = -11.55\,^\circ\mathrm{K}$. The one-dimensional Heisenberg model has not been solved exactly. Bonner and Fisher[22] used exact results for rings of a small number of atoms and extrapolated to $N=\infty$, Blöte[23] and de Neef, Kuipers, and Kopinga[24] have used this method with small rings and chains to obtain numerical values of C/R which include the case of $S=\frac{3}{2}$ with antiferromagnetic interactions. In Table VI the values for the Heisenberg model are calculated from numerical tables of Blöte[23(a)] with $S=\frac{3}{2}$ and $J/k=-9.81\,^\circ\mathrm{K}$. The calculations of de Neef[24(b)] give at 10 °K a value C/R about 25% higher than listed. His remaining values agree with Blöte to within two percent.

Except at 10 °K, where the tail of the peak at 7 °K will contribute and where the theoretical estimates for the Heisenberg model are uncertain, the observed values of (C/R)(mag) of VF_2 are intermediate between the Ising and Heisenberg models but much closer to the latter. Blöte[23(b)] has calculated that a nonzero D raises the heat capacity in the neighborhood of the maximum. We conclude that the magnetic heat capacity of VF_2 is well represented by a Heisenberg linear chain, with antiferromagnetic exchange interactions, and with long-range ordering caused by relatively weak interactions between chains.

Three values of the exchange constant J can be obtained from our data. (1) From $E(\mathrm{mag}) = 101 \pm 5$ cal mole^{-1} and $E(\mathrm{mag})/NJ = 5.67 \pm 0.02$ calculated by Blöte[23(a)] one obtains $J/k = -9.0 \pm 0.5\,^\circ\mathrm{K}$. (2) From the temperature of the maximum in heat capacity, $26.8 \pm 1.0\,^\circ\mathrm{K}$, and the calculated[23,24] values of J/kT, $J/k = -9.7 \pm 0.4\,^\circ\mathrm{K}$. (3) From the high temperature limit of the heat capacity for a Heisenberg linear chain, $C/R = 4J^2S^2(S+1)^2/(3kT)^2$, and the value $A = 2.6 \pm 0.5$ cal °K mole^{-1}, $J/k = -8.4 \pm 1.5\,^\circ\mathrm{K}$. A weighted mean is $J/k = -9.4 \pm 0.4\,^\circ\mathrm{K}$.

In the ordered magnetic structure[25] of VF_2 the spins lie perpendicular to the c axis and spiral about it with a turn angle of $96.0^\circ \pm 0.5^\circ$. From the theory of Yoshimori[26] $J_2/J_1 = 0.10$ and therefore $J_2/k = -0.9 \pm 0.1\,^\circ\mathrm{K}$. A less accurate value of $J_1/J_2 = 6$ was deduced[19] from the low-temperature anisotropy of the magnetic susceptibility. By a Green's function method Takeuchi[27] has recently calculated $J_2/J_1 = 0.156$ for VF_2. With this value $J_2/k = -1.5\,^\circ\mathrm{K}$. In the ordered magnetic structure adjacent spins along the c axis are nearly antiparallel. In a structure where the neighboring spins of chains along the c axis were strictly antiparallel the net effect of the J_2 interactions would vanish since a V^{2+} ion sees four spins in the $[\pm 1, \pm 1, 1]$ directions with spin opposite to the four in the $[\pm 1, \pm 1, -1]$ directions. The spiral structure minimizes the total energy by a relaxation of the antiparallel orientations in chains along [001] to gain energy from the eight neighbors with an antiferromagnetic J_2. Since there is a large short-range correlation from J_1, the J_2 interactions have a much smaller effect than would be guessed from the magnitude of J_2/J_1 and the ordering temperature of 7 °K is at a temperature low compared to the maximum in the heat capacity.

ACKNOWLEDGMENTS

This work was supported by the National Science Foundation. We have benefited from facilities provided by the Advanced Research Project Agency for Materials Research at the University of Chicago. We thank the Vanadium Corporation of America for the gift of vanadium metal. We thank Miss Myrtle Batchelder for the chemical analyses and Dr. D. W. Osborne for computer programs.

[1] W. O. J. Boo and J. W. Stout, J. Chem. Phys. **65**, 3929 (1976).
[2] E. Catalano and J. W. Stout, J. Chem. Phys. **23**, 1803 (1955).
[3] E. Catalano and J. W. Stout, J. Chem. Phys. **23**, 1284 (1955).
[4] J. W. Stout and E. Catalano, J. Chem. Phys. **23**, 2013 (1955).
[5] W. O. J. Boo and J. W. Stout, J. Chem. Phys. **71**, 9 (1979), following paper.
[6] H. J. Seifert and B. Gerstenberg, Angew. Chem. **73**, 657 (1961).
[7] J. W. Stout and W. O. J. Boo, J. Appl. Phys. **37**, 966 (1966).
[8] M. W. Shafer, Mater. Res. Bull. **4**, 905 (1969).
[9] C. Cros, R. Feurer, and M. Pouchard, J. Fluorine Chem. **7**, 605 (1976).
[10] B. M. Wanklyn, B. J. Gerrard, F. Wondre, and W. Davison, J. Cryst. Growth **33**, 165 (1976).
[11] (a) M. Griffel and J. W. Stout, J. Am. Chem. Soc. **72**, 4351 (1950); (b) J. W. Stout, and S. A. Reed, J. Am. Chem. Soc. **76**, 5279 (1954).
[12] W. S. McCain, D. L. Albright, and W. O. J. Boo, Advan. X-Ray Anal. **14**, 433 (1971).
[13] K. Haefner, Ph. D. thesis (unpublished), University of Chicago, 1964.
[14] C. S. Barrett, *Structure of Metals*, 2nd ed. (McGraw-Hill, New York, 1952), p. 618.
[15] A. G. Cole, J. O. Hutchens, R. A. Robie, and J. W. Stout, J. Am. Chem. Soc. **82**, 4807 (1960).
[16] W. J. de Haas and J. de Boer, Physica (The Hague) **1**, 609 (1934).
[17] W. O. J. Boo, Ph.D. thesis (unpublished), University of Chicago, 1966.
[18] J. W. Stout, in *Experimental Thermodynamics Vol. I Calorimetry of Nonreacting Systems*, edited by J. P. McCullough and D. W. Scott (Butterworths, London, 1968), Chap. 6.
[19] J. W. Stout and H. Y. Lau, J. Appl. Phys. **38**, 1472 (1967).
[20] M. Peter and J. B. Mock, Phys. Rev. **118**, 137 (1960).
[21] (a) E. Ising, Z. Phys. **31**, 253 (1925); (b) C. F. Newell and E. W. Montroll, Rev. Mod. Phys. **25**, 353 (1953).
[22] J. C. Bonner and M. E. Fisher, Phys. Rev. Sect. A **135**, 640 (1964).
[23] (a) H. W. J. Blöte, Physica (Utrecht) **78**, 302 (1974); (b) H. W. J. Blöte, Physica (Utrecht) **79B**, 427 (1975).
[24] (a) T. de Neef, A. J. M. Kuipers, and K. Kopinga, J. Phys. A: Math. Nucl. Gen. **7**, L 171 (1974); (b) T. de Neef, Phys. Rev. B **13**, 4141 (1976).
[25] H. Y. Lau, J. W. Stout, W. C. Koehler, and H. R. Child, J. Appl. Phys. **40**, 1136 (1969).
[26] A. Yoshimori, J. Phys. Soc. Jpn. **14**, 807 (1959).
[27] S. Takeuchi, J. Phys. Soc. Jpn. **37**, 809 (1974).